Int. Agrophysics, 1995, 9, 83-93

DIRECTIONAL CHARACTER OF SOIL SURFACE REFLECTANCE IN THE VISIBLE AND NEAR-INFRARED RANGE

J. Cierniewski[1], *M. Verbrugghe*[2], *S. Białousz*[3], *J. Chmiel*[3]

[1] Institute of Physical Geography, University of Poznań, Fredry 10, 61-701 Poznań, Poland
[2] INRA, Station de Bioclimatologie, Centre de Recherches d'Avignon, 84-140 Montfavet, France
[3] Institute of Photogrammetry and Cartography, Warsaw University of Technology
Politechniki Square 1, 00-661 Warsaw, Poland

Accepted February 28, 1995

A b s t r a c t. The paper shows the importance of directional effects on soil reflectance in the visible and near -infrared range. It includes physical principles of surface interactions with radiation in this spectral range, and examples of soil reflectance measurements performed during Polish-French cooperation.

K e y w o r d s: soil surface reflectance, bidirectional reflectance distribution function, remote sensing

INTRODUCTION

Soils, as most natural surfaces, have non-Lambertian reflectance properties. Soil surfaces seem to be the brightest from the direction which gives the lowest proportion of shaded fragments. The Sun is then behind the back of a person or a sensor looking at these surfaces, and their viewing direction approximates to the incidence angle of the sunbeams. If the sunbeams not only scatter from a soil diffusely, but also are partly specularly reflected, this phenomenon becomes less visible as a result of soil self-shadowing. Specific objects, like very smooth soils or flat salt soils, and vegetation with very brilliant leaves, seem to be the brightest when they are observed towards the Sun, especially at its low position. When these surfaces are horizontally positioned, then are viewed at the maximum of their brightness at the same angle as the sunbeam incidence angle, but from the opposite direction.

When analysing those non-Lambertian objects using remote sensing data collected at the ground, air or space levels, we have to know that their spectral properties depend on the position of the Sun as well as on the position of a sensor. The knowledge of the bidirectional reflectance distribution function of a given object is necessary to make the analysis precise. This function enables a quantitative comparison of spectral data collected in different illumination and observation conditions. It is especially important in the context of satellite images formed by scanners viewing surfaces at wide scan angles, as the Advanced Very High Resolution Radiometer (AVHRR) of the NOAA satellites, or scanners with a variable viewing angle, as the High Resolution Visible (HRV) instrument of the SPOT satellites.

The aim of this paper is to present characters of soil directional reflectance in the visible and near-infrared range. They include physical principles of surface interactions with radiation in this spectral range, and examples of soil reflectance measurements performed during Polish-French cooperation.

SURFACES INTERACTIONS WITH ELECTROMAGNETIC RADIATION

Information about interpreted objects in remote sensing methods in the visible and near-infrared range is transmitted by electromagnetic radiation reflected from surfaces of these objects. The character of the reflection is described by Rayleigh's criterion of surface roughness:

$$h \leq \lambda/(8 \cos \theta_i) \qquad (1)$$

where h - height variations above a plane in wavelength (λ), θ_i - angle of incidence from the normal to the surface [16].

When h satisfies this criterion, the surface is smooth and specular reflection occurs. Otherwise, it is rough and diffuse reflection appears. According to Eq. (1), the critical size of h changes considerably not only with the wavelength (λ), but also with the angle of incidence (θ_i). Taking into account the extreme wavelengths of the visible and near-infrared range (0.36 and 1.3 μm) for θ_i = 10°, 50°, and 70° those critical values amount, respectively, to 0.05, 0.07 and 0.13 μm for the low wavelength value and to 0.17, 0.25, and 0.47 μm for the high one. Each of the calculated values of h corresponds to a size of clay soil material, the equivalent diameter of which is defined as less than 2 μm.

Specular reflection meeting the criterion of smooth surfaces given above manifests high directivity. The angle of the reflected wave equals the angle of the incident wave. Not all radiation striking smooth surfaces is reflected (ρ_λ). The spectral radiant flux (ψ_λ), defined as the total energy radiated by a unit area in all directions in a unit of time within the wavelength band (λ), is the sum of reflected (ρ_λ), absorbed (α_λ) and transmitted (τ_λ) energy [8]. Most of electromagnetic energy in the discussed range coming to a soil surface is absorbed and reflected. Only a very small part of it is transmitted for partially transparent soil material. Reflection from a grainy soil material occurs mainly from external surfaces of the particles.

Diffuse reflection, a characteristic of rough surfaces by Rayleigh's criterion, scatters incident radiation in all directions. The intensity of reflected electromagnetic radiation ($I_{(\theta)}$), defined as total energy per solid angle of measurement, is directly proportional to the intensity of incident radiation (I_o) and the cosine of the angle from the perpendicular (θ) [16]. The intensity of the diffuse reflection, irrespective of the incidence angle of the ray, reaches a maximum at a direction perpendicular to the surface, and equals 0 at a direction parallel to it [26].

The pattern of reradiation of natural surfaces, wholly illuminated by direct radiation and usually neither perfectly smooth nor rough reflectors by Rayleigh's criterion, depends on the proportion between the two size categories of microirregularities. If the surfaces consist mostly of facets larger than the irregularities defined in Eq. 1, the reradiation pattern of a rough surface is similar to the nondirective Lambertian distribution. When they are also composed of partly transparent, relatively large, smooth and polished facets, their reradiation can assume a more directive pattern (Fig. 1).

If position of irregularities of a rough surface makes it impossible to illuminate the whole surface directly, its shadowing becomes another important factor influencing the shape of the surface reradiation pattern [3,4,7,13, 14,19,22,24]. The degree of surface shadowing depends on the density of those elements which cast the shadow, the microconfiguration of the surface, and its slope in relation to the incident rays.

PARAMETERS OF SOIL BIDIRECTIONAL REFLECTANCE

Spectral radiance (L) is the best parameter which describes what is actually measured by a sensor. It is the energy within a given wavelength band radiated by a unit area per unit solid angle of measurement [W m^{-2} sr^{-1} μm^{-1}]. If a Lambertian surface, positioned horizontal, is observed remotely, it shows a hemispherical distribution of reradiation, and seems to be independent of the view angle. Every surface

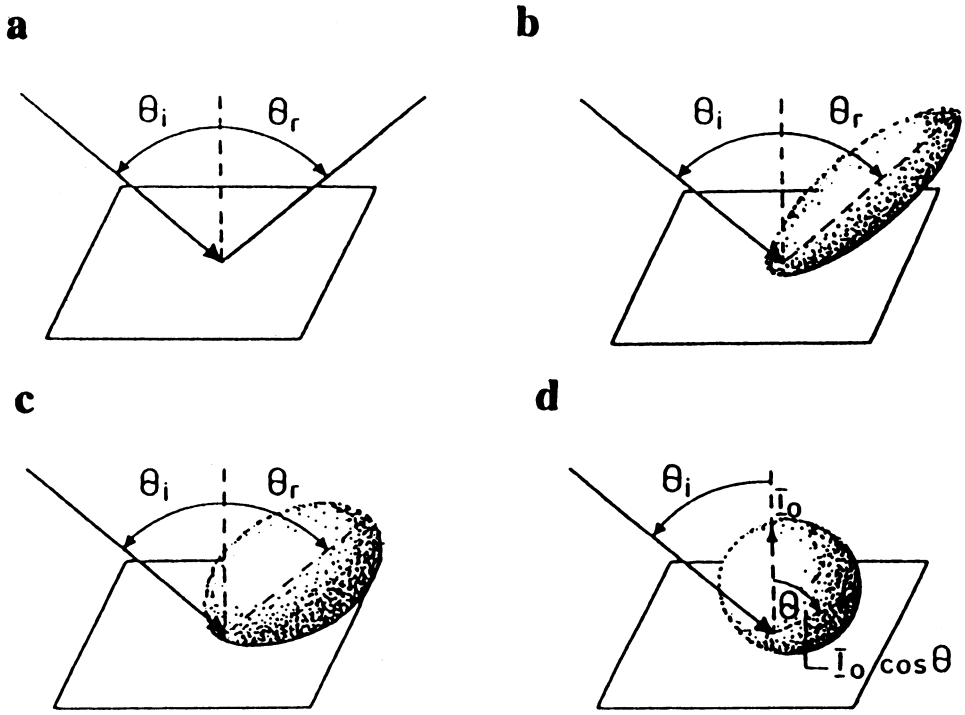

Fig. 1. Distribution of reflected radiant flux from different types of reflecting surfaces: perfect specular (a), near-perfect specular (b), near-perfect diffuse (c) and perfect diffuse (d).

which is characterized by a distribution of reradiation other than the pattern of a horizontal Lambertian surface, is viewed as a surface of non-hemispherical distribution. The reason for this non-Lambertian distribution is roughness by Rayleigh's criterion as well as the shadowing of the surface, varying with the view angle, and also the slope of the surface [6].

Nicodemus *et al.* (cited in [12]) proposed in 1977 a complete description of reradiation from a surface point at all possible angles and called it the bidirectional reflectance distribution function (BRDF):

$$\mathrm{BRDF}_{i,r} = f_r(\Omega_i, \Omega_r) = \frac{dL(\Omega_i, \Omega_r)}{dE(\Omega_i)} \quad (2)$$

where dL - reflected radiance per unit solid angle, and dE - irradiance per unit solar angle.

The two radiation environments, depending on the direction of incidence of radiation from the Sun (Ω_i) and the direction of reflected radiance coming to a sensor (Ω_r), are defined by two angles (Fig. 2). The first, vertical, is called the zenith angle. It denotes the solar zenith angle and is symbolized as θ_s,

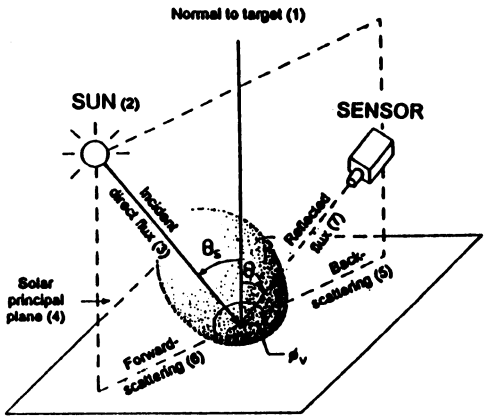

Fig. 2. Geometric relationship between the Sun, target, and sensor positions (modified from Cierniewski and Caurault [5]).

and the view zenith angle symbolized as θ_v. The second one, horizontal, called the azimuth angle, indicates the view azimuth angle as φ_v, relative to the Sun position. Any view direction (Ω_r) is described by a vector towards the sensor, defined with the zenith angle between 0o (nadir view) and 90° (grazing view), and the view azimuth angle between 0° (viewing the forward scattering of solar radiation) and ±180° (viewing the backscattering). The term 'bidirectional' in the context of the BRDF refers to the description of the angular position of two elements, i.e., the source of radiation and the sensor [20].

The BRDF is very difficult to measure in natural conditions. It disregards the diffuse component in illumination. Therefore it is replaced with the bidirectional reflectance factor (BRF). The BRF is defined as the radiance of the target (dL_t) per unit solid angle multiplied by a correction factor and divided by the radiance which would be reflected into at the same solid angle by a perfect Lambertian panel (dL_p), both under the same illumination and viewing conditions [20]. The BRF factor, measured in field condition, includes direct solar radiation as well as diffuse sky-light. Thus, using the factor instead of the BRDF, we should take into account proportion between direct and diffuse radiation in the downwelling radiance, and decide on replacement if sky-light makes a small contribution to total radiation. For an aerosol-free atmosphere, the diffuse component reaching thc surface in the visible range is about 3 % of the total flux, while for a moderate aerosol load (at the horizontal visual range V_o=23 km) and for a heavy load (at V_o = 5 km) it is, respectively, 26 % and 64 % of the total [25]. Within the visible and near-infrared range, the contribution of sky-light decreases with the wavelength. Measurements of Yost and Wenderoth (1969) [in 21] show that the diffuse/direct radiation ratio is the highest (45 %) for about 400 nm. For 450 and 550 nm it is 20 % and 10 %, respectively. Then, up to about 1 000 μm, it stabilizes at about 5 %.

MEASUREMENTS OF SOIL BIDIRECTIONAL REFLECTANCE

Distribution of reflected energy

The soil bidirectional reflectance in the visible and near-infrared range has mainly been discussed as a background for spectral response of vegetative surfaces [1,2,8-11,14, 18,19,23]. Remotely sensed data on the soil surface, like vegetation canopies, demonstrate non-Lambertian reflectance properties.

Rough soil surfaces usually display a backscatter reflectance peak towards the position of the Sun, and decreasing reflectance in the direction away from this peak, with minimum reflectance in the extreme forwardscatter direction near the horizon (Figs 3-6). Nearly bare soils of different surface roughness collected by Kimes and Sellers [17] exhibit those reflectance pattern. They were measured in two spectral bands (0.58-0.68 μm and 0.73-1.1 μm), using field radiometer, recording reflectance in 41 directions at view zenith angles ranging from 0° to 75° in 15° increments and the view azimuth angles from 0° to 315° in 45° increments. Milton and Webb [19] presented results of airborne and ground measurements of the reflectance of bare soils, indicating the angular asymmetry of reflectance around the nadir in the solar principal plane (SPP). Figure 2 explaines position of the plane. When examining the influence of cultivation practices on the direct reflectance of sandy soils of different moisture, the authors observed that ploughing considerably decreased soil reflectance. It was the effect of the increase in soil surface moisture, as well as in soil surface roughness. They also found that the peak of backscatter radiation became less pronounced at a low solar zenith angle.

Irons and Smith [15] show that the roughest soil surface of a fine-loamy texture, ploughed with a mouldboard plough, scattered radiation forward as strongly as the smoothest surface obtained by tilling with a disk plough and then compacting to create a smoother surface. The relatively larger shadowing of the roughest soil in compensation for its strong forward-scatter was given as the reason of the effect.

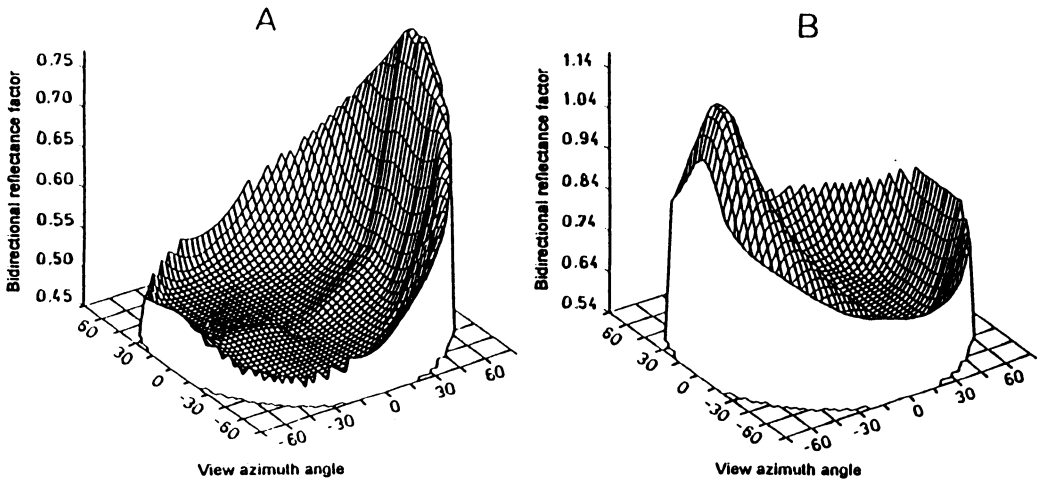

Fig. 3. Three-dimensional polar plots of the bidirectional distribution of reflectance in the red wave for: alkali soil (A) and dune sand (B) flat at 68° and 69° solar zenith angles, respectively (modified from [9]).

It was possible to detect it by taking very detailed field spectral measurements in six of the bands corresponded to the TM bands, and the seventh to the middle infrared one (1.15-1.3 μm). Radiance was measured from the soil at view azimuth angles ranging from 0° to 315°, relative to the solar principal plane in 45° increments, and at view zenith angles ranging from 0° to 70° in 10° increments. Deering *et al.* [9] have supplied evidence that soil reflectance can clearly indicate the backscatter as well as the forwardscatter regime (Fig. 3). They have demonstrated it on the examples of an alkali flat bare soil and a dune sand surface, using a three-channel (0.65-0.67, 0.81-0.84 and 1.62-1.69 μm) field radiometer, called PARABOLA. It collects radiance data from an almost complete sky- and ground-looking hemispheres in 15° field-of-view sectors. The first surface (Fig. 3A), of coarse texture and bright stabilized crust with intermittent darker patches, displayed the distribution pattern of strong backscatter reflectance. The second surface (Fig. 3B), composed of nearly pure gypsum crystals creating uniform wind ripples, showed forwardscatter as its predominant feature.

Polish-French studies

The examples of the distribution of the bidirectional reflectance factor, presented in Fig. 3, show that the highest variations in soil reflectance are recorded along the solar principal plane (SPP), whereas the lowest ones - in the plane perpendicular to it (PP). Measurements of soil bidirectional reflectance, performed in Polish-French cooperation, mainly concentrated on these two planes.

Measurements collected in France in 1991 and 1992 were used for verification and evaluation of the accuracy of mathematical models predicting the reflectance of rough soil surfaces [6,27]. The models simulate soil surfaces by equal-sized spheroids of a given proportion of their vertical to horizontal radii, laying on a horizontal plane. They are arranged on it in such a way that their centres in the horizontal projection are at a given distance, indepedently of the azimuthal position of the solar principal plane. This regularity in the spacing of the spheroids expresses isotropic features of the geometry of the simulated soil surface. The models assume that wave energy in the visible and near-infrared range reflected from the soil surface is strongly correlated with the area of its sunlit fragments and significantly reduced

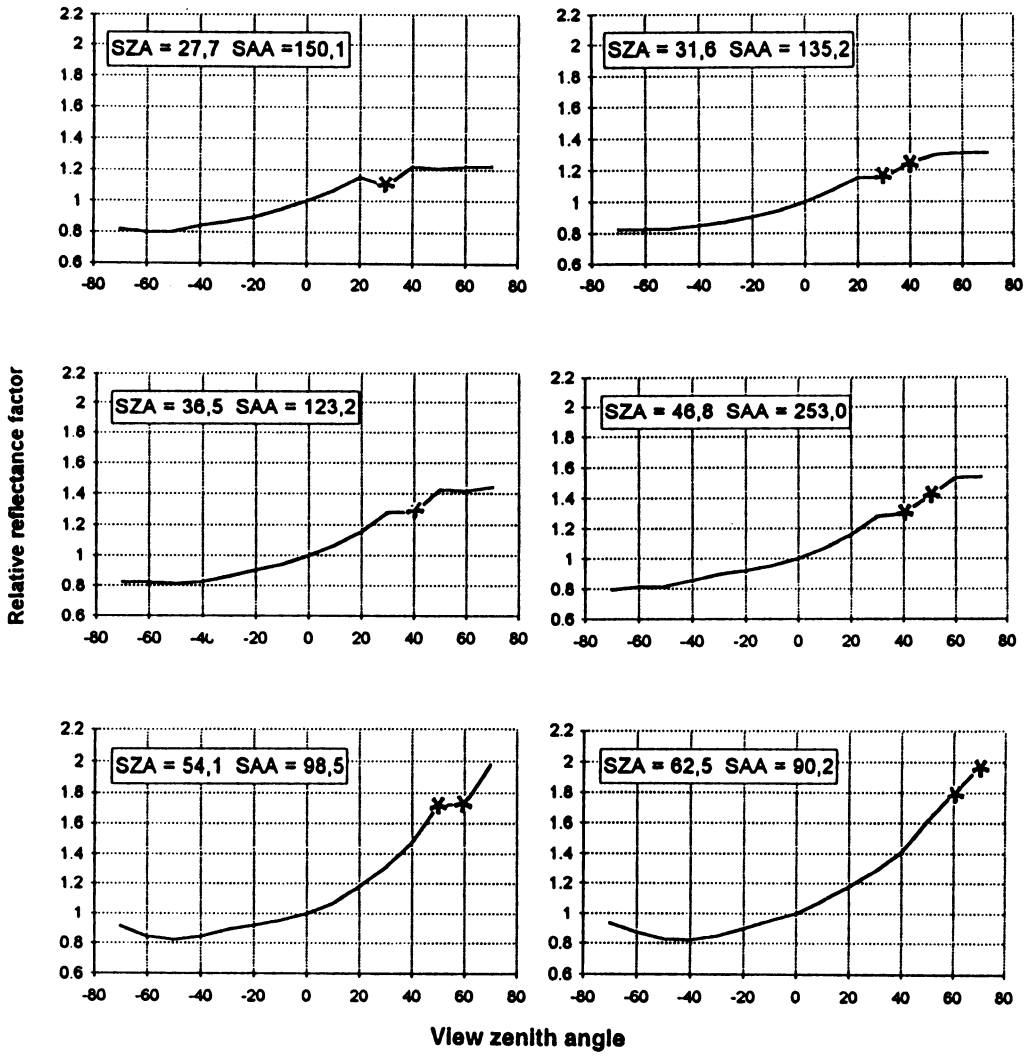

Fig. 4. Reflectance curves of the surface with pebbles along the solar principal plane for the channel SX2 of the CIMEL radiometer for selected solar zenith angles (SZA). SAA is the solar azimuth angle, * - measured reflectance data collected when the radiometer cast a shadow on the observed surface.

by the area of its shaded fragments. Furthermore, the energy leaving the sunlit fragments is directly proportional to the energy coming to them, that is, it also depends on the angle of incidence of the sunbeams on those directly illuminated parts. The accuracy of the soil reflectance distribution in the view zenith angle function generated by the models was tested on a geometrically uncomplicated soil surface. It was a bare field on the alluvial plain of the Rhone river, named la Crau, located 40 km to the south of Avignon, and 15 km north of the Mediterranean Sea. The plain is covered with regularly spread pebbles of an average diameter of several centimeters. A medium-textured soil, partly overgrown by natural vegetation, appears between the stones. This area serves as a winter pasture for sheep.

The bidirectional reflectance measurements along the principal plane, presented here in the form of the relative reflectance factor (as the off-nadir to nadir reflectance ratio), also show

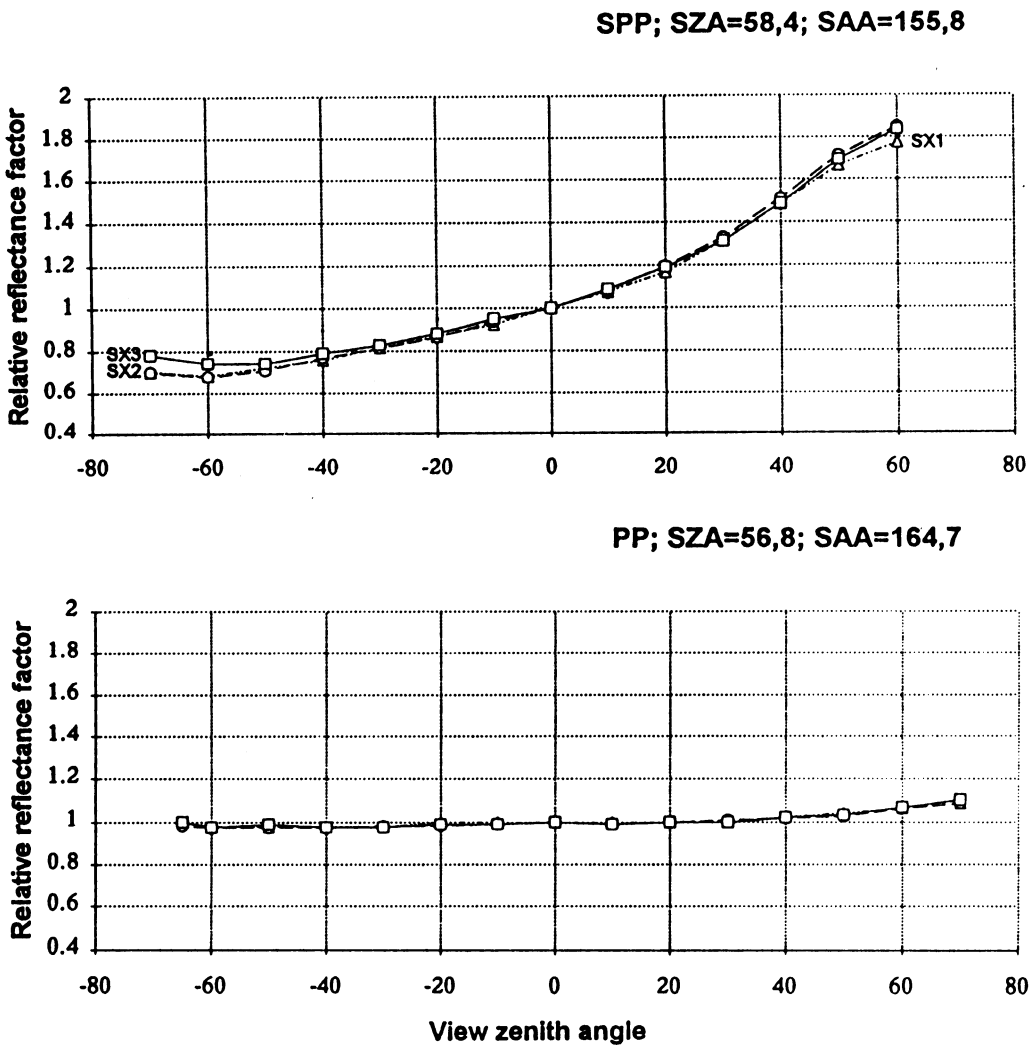

Fig. 5. Reflectance curves of the bare soil lessivé along the solar principal plane (SPP) and the perpendicular plane (PP). SZA is the solar zenith angle and SAA is the solar azimuth angle.

effects of specular reflection (Fig. 4). The lower the Sun position, the more they are visible. Variation in the soil reflectance along the solar principal plane increases with a decreasing solar position.

The measurements of soil bidirectional reflectance, carried out in Poland in September and October 1992 were used to analyse bidirectional reflectance with different proportion of the vegetation cover. The measurements were collected in fields near Warsaw. Examples of the relative reflectance factor from a bare soil lessivé (Fig. 5) and the same soil run a little to weeds (Fig. 6), both in almost the same illumination conditions, show a wider variation in the factor when the soil is covered by weeds. The influence of the vegetation cover on the reflectance distribution along the solar principal plane seems to be significant if we compare the different reflectance distributions of the two surfaces with their degree of weed cover (Photo 1A and 1B). The distributions of the relative reflectance factor for a field of carrot, measured in the planes situated

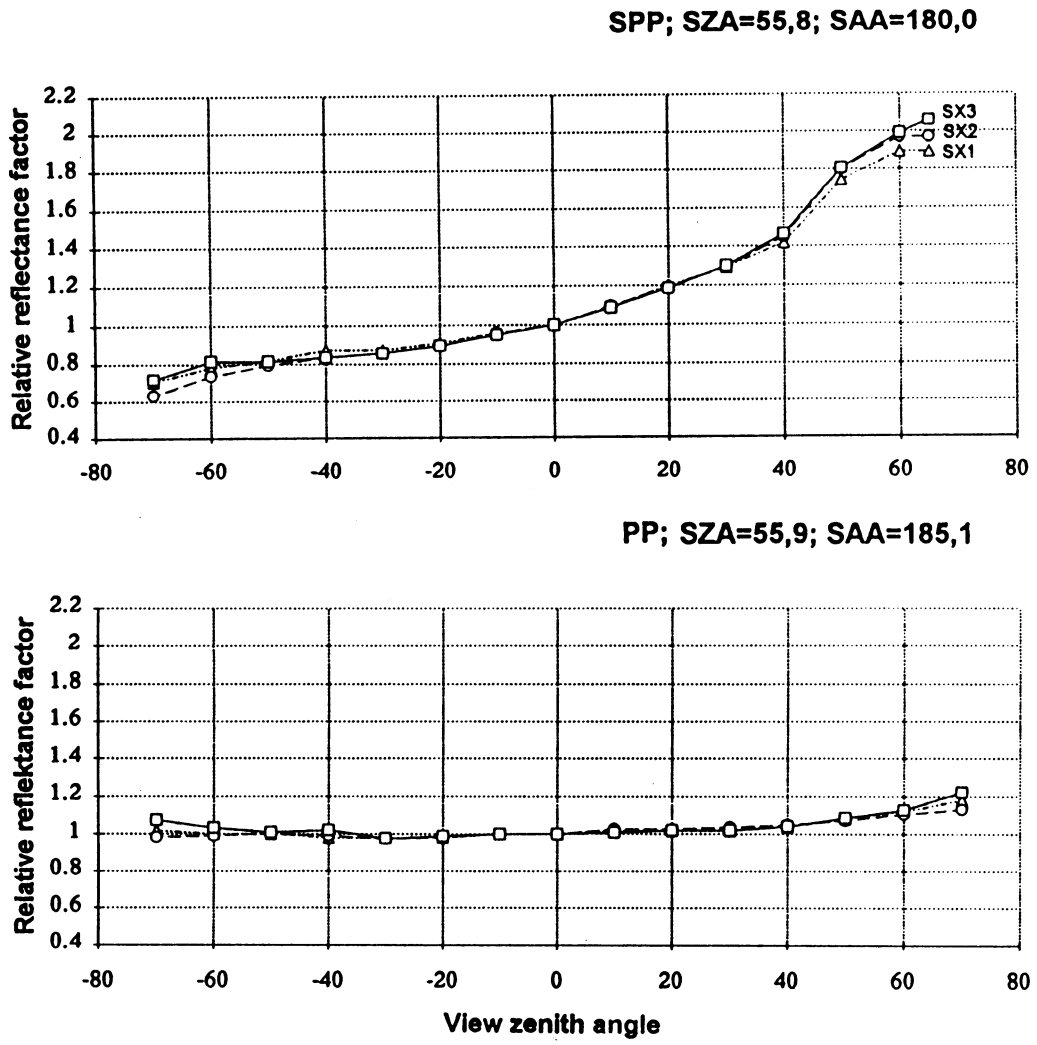

Fig. 6. Reflectance curves of the soil lessivé, run a little to weeds, along the solar principal plane (SPP) and the perpendicular plane (SPP). SZA is the solar zenith angle and SAA is the solar azimuth angle.

approximately in the solar principal plane (~SPP) and the perpendicular one (~PP), have quite a different character (Fig. 7). The features typical of crop vegetation start to dominate in these characteristics. A general shape of the crop, cylindrical in this example (Photo 1C), crucially determines the crop reflectance distribution shape [27].

Measurements

The spectral measurements presented in the paper were collected in France and Poland by a three-channel (SX1: 0.50-0.59 μm, SX2: 0.61-0.68 μm and SX3: 0.79-0.89 μm) field radiometer CIMEL simulating the SPOT (HRV) bands. It recorded radiance data in 15 directions at view zenith angles from 70° towards the Sun through the nadir (0°) to 70° away from the Sun at 10° increments. The duration of a complete sequence was about 4 min. The radiometer observed the soil surface from a distance of 2 m. This instrument with a 12° field-of-view integrated reflected energy from a circular area of 0.14 m^2 at a 0° view zenith

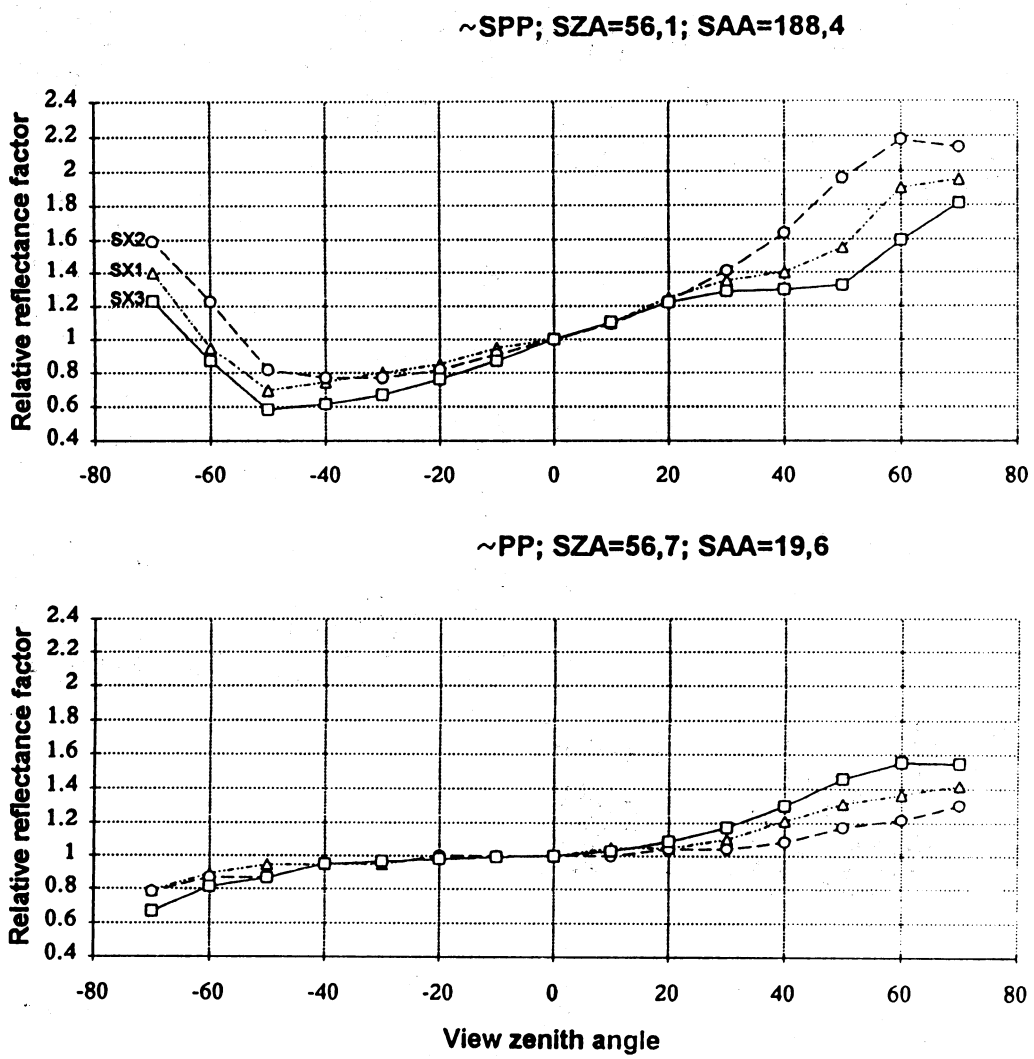

Fig. 7. Reflectance curves of the field of the carrot, near the solar principal plane (~SPP) and near the perpendicular plane (~PP). SZA is the solar zenith angle and SAA is the solar azimuth angle.

angle to an elliptical area of 0.44 m^2 at a 70° view zenith angle.

FINAL REMARKS

The distribution of soil bidirectional reflectance in the visible and near-infrared range depends on a micro- and macro-structure of a soil surface. The size and orientation of the smallest irregularities of a soil particle surface determines the character of reflection of the sunbeams directly illuminating soil surface fragments. These irregularities determine the proportion of the diffuse and the specular components in the total reflection of electromagnetic energy of a given wavelength. However, the main reason of the non-Lambertian behaviour of soil surfaces is the significance of these irregularities as elements producing shadow areas on the surface, larger or smaller in relation to the zenithal position of the Sun. Thus, the geometry of a soil surface, as well as the position of the Sun and of the sensor,

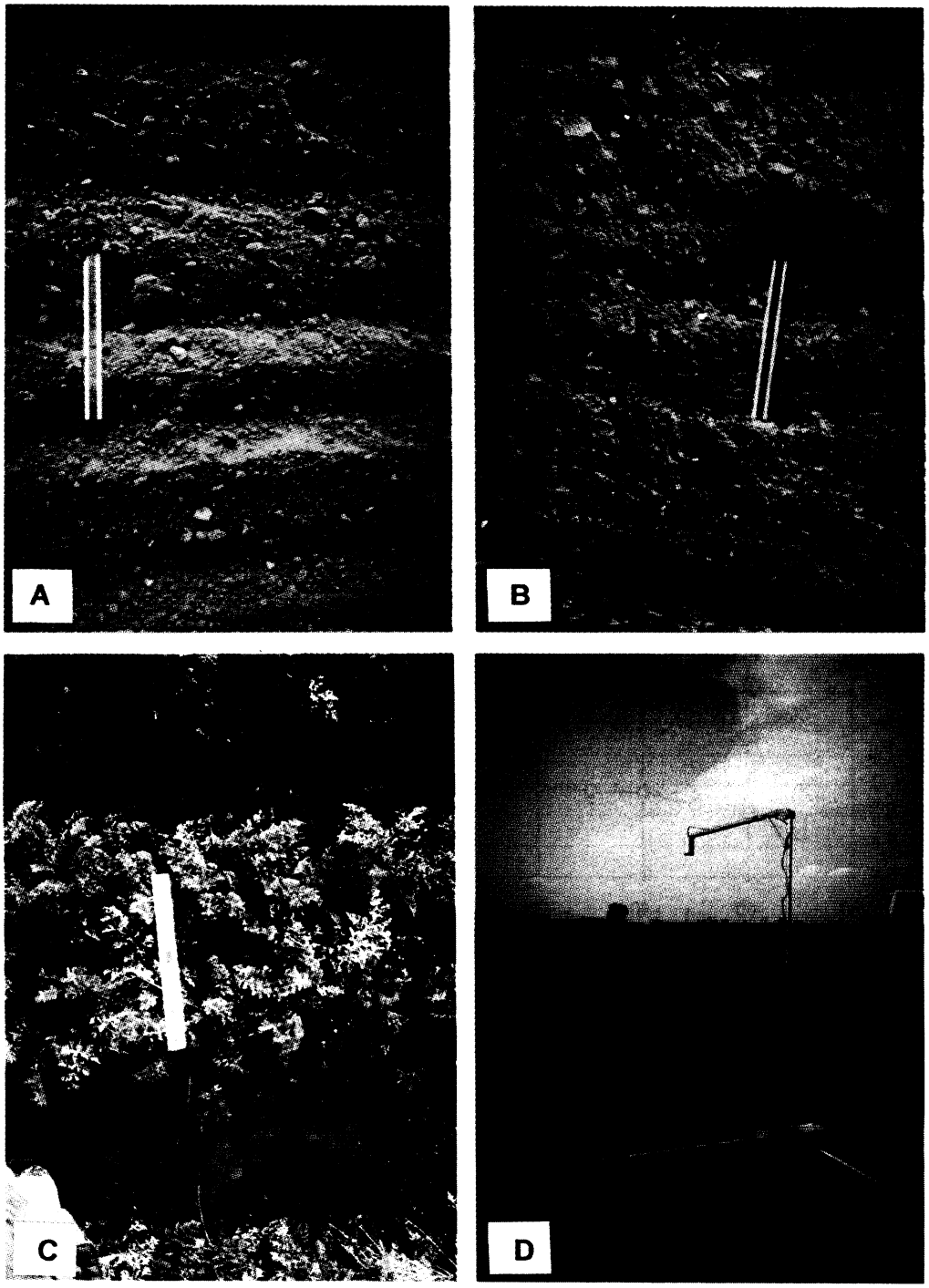

Photo 1. Surfaces characterized spectrally: the bare soil lessivé (A), the soil lessivé run a little to weeds (B), the field of the carrot (C); the ruler lying on the surface is 30 cm long, and the CIMEL radiometer ready to the bidirectional reflectance measurements (D).

determine of the soil image recorded by remote sensing methods.

The results of the soil bidirectional reflectance studies presented in this paper demonstrate that by ignoring the influence of soil illumination and observation conditions on their remotely sensed data, we can commit a grave error in their interpretation.

REFERENCES

1. **Bartlett D.S., Johnson R.W, Hardisky M.A, Klemas V.:** Assessing impacts of off-nadir observation on remote sensing of vegetation: Use of the Suits model. Int. J. Rem. Sens., 7, 247-264, 1986.
2. **Brennan B., Bandeen W.R.:** Anisotropic reflectance characteristics of natural Earth surfaces. Appl. Opt., 9, 405-412, 1970.
3. **Clerniewski J.:** A model for surface roughness influence on the spectral response of bare soils in the visible and near-infrared range. Rem. Sens. Env., 23, 99-115, 1987.
4. **Clerniewski J.:** The influence of the viewing geometry of bare rough soil surfaces on their spectral responses in the visible and near-infrared range. Rem. Sens. Env., 27, 135-142, 1989.
5. **Clerniewski J., Caurault D.:** Bidirectional reflectance of bare soil surfaces in the visible and near-infrared range. Rem. Sens. Rev., 7, 321-339, 1993.
6. **Clerniewski J., Verbrugghe M.:** A geometrical model of soil bidirectional reflectance in the visible and near-infrared range. Proc. 6th Int. Symp. 'Physical Measurements and Signatures in Remote Sensing'. Val d'Isere, France, 635-642, 1994.
7. **Cooper K.D, Smith J.A.:** A Monte Carlo reflectance model for soil surfaces with three-dimensional structure. IEE Trans. Geosci. Rem. Sens., GE-23, 668-673, 1985.
8. **Curran P.J.:** Earth surface interactions with electromagnetic radiation. In: Principles of Remote Sensing. Longman Ed., London and New-York, 1985.
9. **Deering D.W., Eck T.F., Otterman J.:** Bidirectional reflectances of selected desert surfaces and their three parameter soil characterisation. Agric. Forest Meteorol., 52, 71-93, 1990.
10. **Eaton F.D., Dirmhirn I.:** Reflected irradiance indicatrices of natural surfaces and their effect on albedo. Appl. Opt., 18, 994-1003, 1979.
11. **Foody G.M.:** The effects of viewing geometry on image classification. Int. J. Rem. Sens., 9, 1909-1915, 1988.
12. **Gerstl S.A.W., Simmer C.:** Radiation physics and modelling for off-nadir satellite-sensing of non-Lambertian surfaces. Rem. Sens. Env., 20, 1-29, 1986.
13. **Graetz R.D., Gentle M.R.:** A study of the relationship between reflectance characteristics in the Landsat wavebands and the composition and structure of an Australian semi-arid rangeland. Photogram. Eng. Rem. Sens., 48, 1721-1736, 1982.
14. **Huete A.R.:** Soil and sun angle interactions on partial canopy spectra. Int. J. Rem. Env., 8, 1307-1317, 1987.
15. **Irons J.R., Smith J.A.:** Soil surface roughness characterization from light scattering observations. 10th Ann. Int. Geosciences and Remote Sensing Symp., II, 1007-1010, 1990.
16. **Janza F.:** Interaction Mechanisms. Manual of Remote Sensing, Am. Soc. of Photogrammetry, Falls Church, Virginia, 1975.
17. **Kimes D.S., Seller P.J.:** Inferring hemispherical reflectance of the Earth's surface for global energy budget from remotely sensed nadir or directional radiance values. Rem. Sens. Env., 18, 205-223, 1985.
18. **Kriebel K.T.:** On the variability of the reflected radiation field due to differing distributions of the irradiation. Rem. Sens. Env., 4, 257-264, 1976.
19. **Milton E.J., Webb J.P.:** Ground radiometry and airborne multispectral survey of bare soils. Int. J. Rem. Sens., 8, 3-14, 1987.
20. **Milton E.J.:** Principal of field spectroscopy. Remote Sens. Yearbook, 1988-1989, 79-99, 1989.
21. **Mulders M.A.:** Remote Sensing in Soil Science. 15, Elsevier, Amsterdam, Oxford, New-York, Tokyo, 1987.
22. **Norman J.M., Welles J.M., Walter E.A.:** Contrast among bidirectional reflectance of leaves, canopies, and soils. IEE Trans. Geosci. Rem. Sens., GE-23, 659-667, 1985.
23. **Ott W., Pfeiffer B., Quiel F.:** Directional reflectance properties determined by analysis of airborne multispectral scanner data and atmospheric correction. Rem. Sens. Env., 116: 47-54, 1984.
24. **Ranson K.J., Biehl L.L., Bauer M.E.:** Variation in spectral response of soybeans with respect to illumination, view and canopy geometry. Int. J. Rem. Sens., 6, 1827-1842, 1985.
25. **Simmer C., Gerstl S.A.W.:** Remote sensing of angular characteristics of canopy reflectance. IEE Trans. Geosci. Rem. Sens., GE-23, 648-659, 1985.
26. **Slater P.:** Photographic systems for remote sensing. Manual of Remote Sensing. Am. Soc. of Photogrammetry, Falls Church, Virginia, 1975.
27. **Verbrugghe M., Clerniewski J.:** Effects of sun and view geometries on cotton. Bidirectional reflectance test of a geometrical model. Rem. Sens. Env. (Special issue), 1995, (in press).